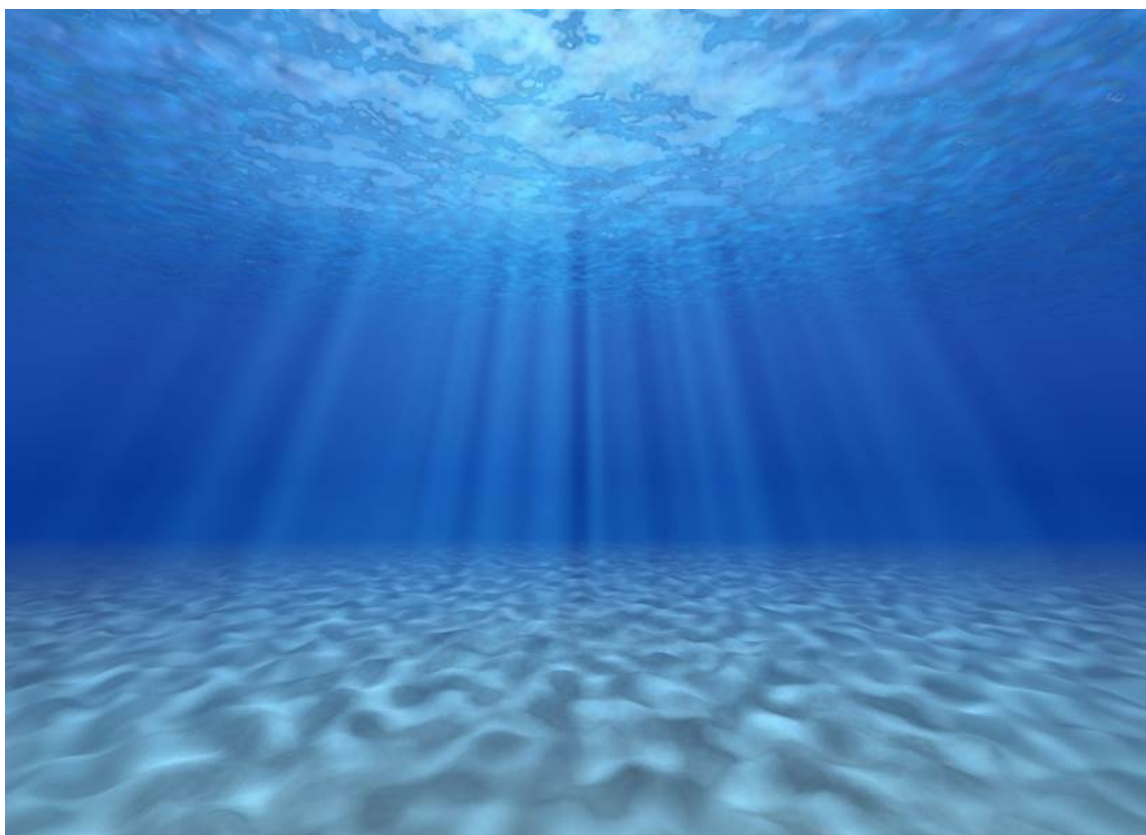


# Sentinel-3 OLCI Inherent Optical Properties

## Algorithm Theoretical Basis Documents

### ATBD



Date: 31 July 2019

EUMETSAT contract: 17/214791

EUMETSAT Ref.: EUM/RSP/REP/20/1160644



## Acronyms

ATBD	Algorithm Theoretical Basis Documents
ESA	European Space Agency
IOPs	Inherent Optical Properties
OLCI	Ocean and Land Colour Imager
WCP	Water classification product
OWT	Optical water types
SVD	Single value decomposition

<b>Symbol</b>	<b>definition</b>	<b>Dimension</b>
Geometry, wavelengths, others		
$\lambda$	Wavelength	nm
$\theta_s$	Sun Zenith Angle	Degrees
$\mu_w$	Cosine of the angle of refraction of the solar beam just beneath the sea surface	
$\eta$	Ratio of molecular scattering to total scattering	
Radiometry and Apparent Optical Properties (AOPs)		
$R_{rs}$	Remote Sensing Reflectance (above water)	sr <sup>-1</sup>
$r_{rs}$	Remote Sensing Reflectance (bellow water)	sr <sup>-1</sup>
$K_d$	Attenuation coefficient for downwelling irradiance	m <sup>-1</sup>
Inherent Optical Properties (IOPs)		
$a(\lambda)$	Total absorption coefficient	m <sup>-1</sup>
$a_w(\lambda)$	Water absorption coefficient	m <sup>-1</sup>
$a_{nw}(\lambda)$	Non water absorption coefficient	m <sup>-1</sup>
$a_{phy}(\lambda)$	Phytoplankton absorption coefficient	m <sup>-1</sup>
$a_{phy}^*(\lambda)$	Phytoplankton specific absorption coefficient	m <sup>2</sup> mg <sup>-1</sup>
$a_{cdm}(\lambda)$	Colored Dissolved Matter absorption coefficient	m <sup>-1</sup>
$a_{CDOM}(\lambda)$	Colored Dissolved Organic Matter absorption coefficient	m <sup>-1</sup>
$b_b(\lambda)$	Total backscattering coefficient	m <sup>-1</sup>
$b_{bp}(\lambda)$	Water backscattering coefficient	m <sup>-1</sup>
$b_w(\lambda)$	Particulate backscattering coefficient	m <sup>-1</sup>
$S$	CDOM spectral slope	m <sup>-1</sup>
$Y$	Particle backscattering slope	m <sup>-1</sup>

## Table of Content

	<u>Page.</u>
1 Introduction .....	6
1.1 Purpose and Scope.....	6
1.2 Algorithm identification.....	6
2 Algorithm Overview .....	6
2.1 Objectives .....	6
3 Algorithm Description .....	7
3.1 Implementation workflow.....	7
3.2 Estimation of the total absorption and backscattering coefficients .....	8
3.3 Water classification approach.....	10
3.4 Estimation of the absorption by phytoplankton and colored dissolved organic matter .....	13
3.5 Estimation of the colored dissolved organic matter .....	14
4 Criteria applied to consider a pixel valid .....	15
5 References.....	16

## 1 INTRODUCTION

### 1.1 Purpose and Scope

This Algorithm Theoretical Basis Document (ATBD) is written for the Level-2 product of aquatic Inherent Optical Properties from the Ocean and Land Colour Instrument (OLCI) on board of the European Commission Earth Observation Sentinel-3 satellite. The purpose of this document is to describe the final algorithm (the “two-step algorithm”) which has been selected, among others after an evaluation procedure, to estimate different Inherent Optical Properties (IOPs) from OLCI observations.

### 1.2 Algorithm identification

The two-step algorithm is identified under reference “EUM/RSP/REP/20/1160644” in the Sentinel-3 OLCI documentation. In this document, it will be referred to as a “two-step semi-analytical algorithm”, 2SAA.

## 2 ALGORITHM OVERVIEW

### 2.1 Objectives

The objective is to derive several bio optical products from the spectrum of OLCI remote sensing reflectance,  $R_{rs}(\lambda)$ . The following products can be derived from 2SAA (bands Oa2 412.5nm and Oa3 442.5nm are abbreviated as 412 and 443nm):

- The diffuse attenuation coefficient for downward irradiance,  $K_d(\lambda)$ , (in  $m^{-1}$ ) at 400, 412, 443, 490, 510, 560, 620, and 665 nm.
- The non-water absorption coefficients,  $a_{nw}$  and particulate backscattering coefficient,  $b_{bp}$ , (in  $m^{-1}$ ) at 400, 412, 443, 490, 510, 560, 620, and 665 nm.
- The absorption by phytoplankton,  $a_{phy}$ , and colored detrital matter,  $a_{cdm}$  at 400, 412, 443, 490, 510, 560, 620, and 665 nm (all in  $m^{-1}$ ).
- The absorption by colored dissolved organic matter,  $a_{cdom}(443)$  (in  $m^{-1}$ )

**The selected products recommended for operational generation are the following:**

- The non-water absorption coefficient,  $a_{nw}$  (443), and particulate backscattering coefficient,  $b_{bp}$  (443)
- The absorption coefficient by colored detrital matter,  $a_{cdm}$  (443)
- The absorption coefficient by phytoplankton,  $a_{phy}$  (443)
- The absorption coefficient by colored dissolved organic matter,  $a_{cdom}$  (443)

- The spectral slope of  $b_{bp}(\lambda)$ ,  $Y$
- The vertical diffuse attenuation coefficient for downward irradiance at 490 nm,  $K_d(490)$
- Optical Water Class (OWC)

Another set of parameters will be provided as measurements of uncertainty:

- The percentage of error during the  $R_{rs}$  reconstruction
- The percentage of uncertainty based of the given water class (fixed)
- A flag addressing the possible failures during the inversion

**For users requiring all IOP products in all OLCI spectral bands, a SNAP plugin will be delivered for processing of these products from operational OLCI Level-2 products:**

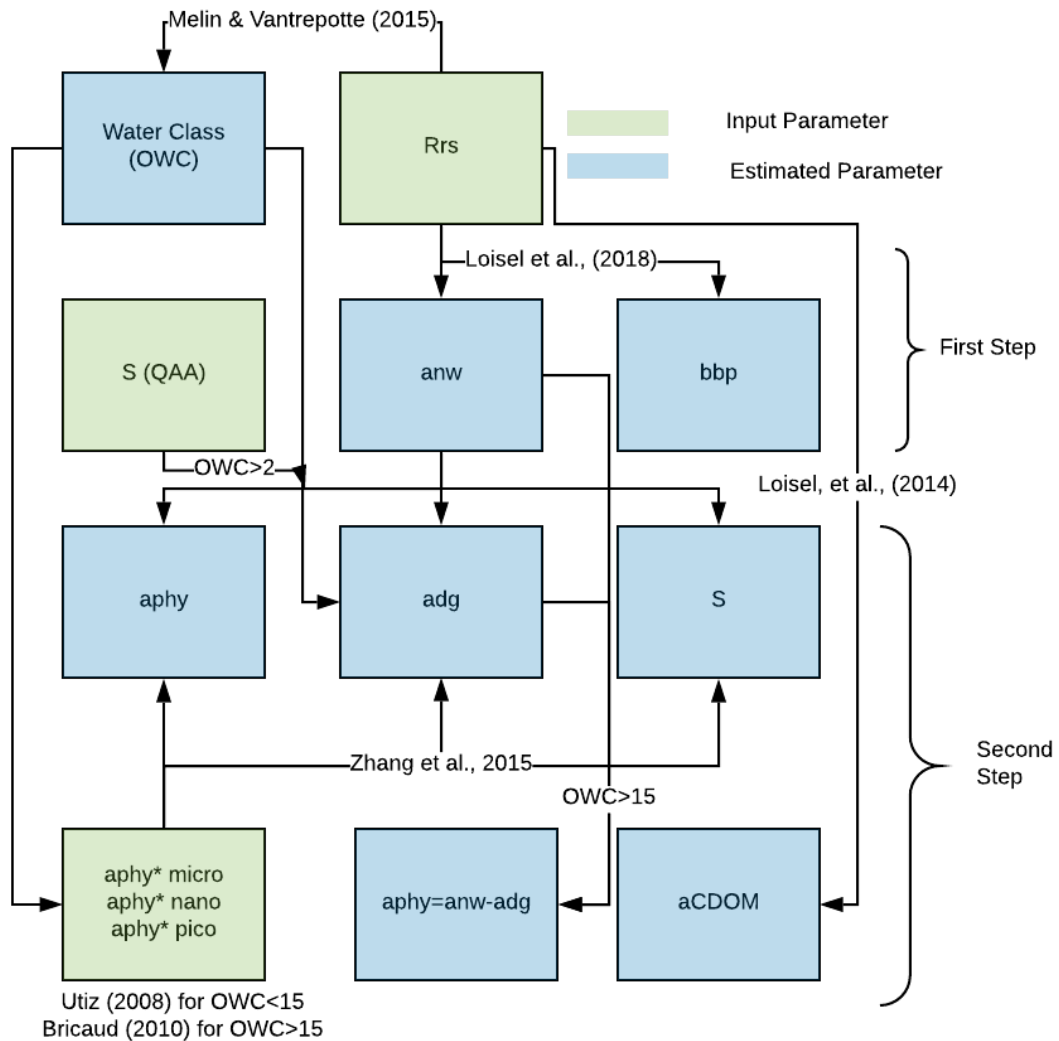
- The non-water absorption coefficient and particulate backscattering coefficient at 400, 412, 443, 490, 510, 560, 620, and 665 nm.
- The vertical diffuse attenuation coefficient for downward irradiance at 490 nm.
- The absorption coefficient by phytoplankton and colored detrital matter at 400, 412, 443, 490, 510, 560, 620, and 665 nm.
- The absorption by colored dissolved organic matter at 443 nm.

### 3 ALGORITHM DESCRIPTION

#### 3.1 Implementation workflow

The general workflow of the algorithm can be divided in two steps. First,  $a_{nw}$  and  $b_{bp}$  will be estimated in the first step from the Loisel et al. (2018) algorithm. Then,  $a_{cdm}$  and  $a_{phy}$  will be estimated in the second step mainly based on the algorithm of Zhang et al., (2015) which has been slightly modified using optical water classes (OWC) (Melin and Vantrepotte, 2015). The original version of the Zhang et al. (2015) algorithm requires the spectral values of  $a_{phy}^*$  for three phytoplankton size classes (pico, nano, micro-phytoplankton), and automatically calculate the spectral shape of  $a_{cdm}$ ,  $S_{cdm}$ . Two different  $a_{phy}^*$  references spectra are used in 2SAA. If the class belongs to 15 or higher (clear waters) the algorithm uses the  $a_{phy}^*$  provided by Bricaud et al. (2010), otherwise the algorithm uses the original  $a_{phy}^*$  from Uitz et al. (2008), as it is used in Zhang et al. (2015). This step is necessary to increase the precision in extremely clear waters. The estimation of  $S_{cdm}$  was also done based on OWC. If the pixel belongs to an optically complex waters (class 1 and 2), the algorithm uses the full Zhang et al. (2015) optimization techniques, otherwise the formulation of Lee et al (2009) to estimate  $S_{cdm}$  is used.

Note that 2SSA only addresses the total phytoplankton absorption, so the  $a_{phy}$  for each size class is not discussed here since it was not tested. Lastly the algorithm also retrieve  $a_{phy}$  in two different ways. If the class is strictly under 15, Zhang et al. (2015) optimization is used, otherwise  $a_{phy}$  is estimated by subtracting  $a_{cdm}$  from  $a_{nw}$ .



### 3.2 Estimation of the total absorption and backscattering coefficients

The proposed algorithm is the “LS2” semi analytical algorithm developed by Loisel et al. (2018). It is the last version of the original LS1 algorithm, proposed in Loisel & Stramski (2000). The LS2 model was developed on the basis of radiative transfer simulations to enable the estimation of two IOPs, the total absorption,  $a(\lambda)$ , and backscattering,  $b_b(\lambda)$ , coefficients within the surface ocean, from the Remote Sensing Reflectance,  $R_{rs}(\lambda)$  ( $\text{sr}^{-1}$ ), and the average attenuation coefficient for downwelling irradiance,  $\langle K_d \rangle_1$  ( $\text{m}^{-1}$ ). It also includes the

correction by Raman scattering by water molecules, which can be significant for clear waters.

The algorithm can be written as:

$$\frac{b_b}{\langle K_d \rangle_1} = f(R_{rs})$$

$$\frac{\langle K_d \rangle_1}{a} = g(R_{rs})$$

where the functions  $f$  and  $g$  depend on the ratio of molecular scattering to total scattering,  $\eta$ , and sun zenith angle,  $\theta_s$ , or equivalently  $\mu_w(\cos(\arcsin(\sin(\theta_s)/1.34)))$ .  $\eta$  is calculated as in Loisel et al. (2018) which requires the chlorophyll-a concentration.

The first equation can be rewritten as:

$$b_b = \langle K_d \rangle_1 [b_{b1}(\eta, \mu_w)R_{rs} + b_{b2}(\eta, \mu_w)R_{rs}^2 + b_{b3}(\eta, \mu_w)R_{rs}^3]$$

Where the coefficients  $b_{b1}$ ,  $b_{b2}$  and  $b_{b3}$  vary as a function of  $\eta$  and  $\mu_w$ .

In the same way:

$$a = \langle K_d \rangle_1 / [a_1(\eta, \mu_w) + a_2(\eta, \mu_w)R_{rs}^1 + a_3(\eta, \mu_w)R_{rs}^2 + a_4(\eta, \mu_w)R_{rs}^3]$$

Where the coefficients  $b_{b1}$ ,  $b_{b2}$  and  $b_{b3}$  vary as a function of  $\eta$  and  $\mu_w$ . Specific values of the coefficients  $a_i$  and  $b_{bi}$  are provided in a look-up-table and an interpolation procedure is applied to calculate these coefficients for intermediate values of  $\eta$  and  $\mu_w$  that are not included in the look-up table.

The last parameter needed for LS2 inversion is the diffuse attenuation coefficient for downwelling radiance ( $\langle K_d \rangle_1$ ). The algorithm of Jamet et al. (2012) is based on a neural network approach which allows the estimation of  $\langle K_d \rangle_1$  at any wavelength between 412 and 670 nm from  $R_{rs}(\lambda)$ . For the LS2, a modified version of Jamet et al. (2012) was implemented, to improve the retrieval accuracy in very oligotrophic and turbid waters. In this case, the model calculates the ratio between  $R_{rs}$  at 490 and 555 nm and if it is lower or equal to 0.85, the neural networks use all  $R_{rs}$  values between 443 and 670 nm as input parameters. In this case, the neural network has two hidden layers with five neurons for each layer. On the other hand, if the  $R_{rs}$  is higher than 0.85, the neural network ignores the red part of the spectrum. In this case, the neural network has two hidden layers with four neurons for each layer. This difference for clear waters is due to the low signal and high signal-to-noise ratio when compared to other bands. For both cases,  $\langle K_d \rangle_1$  is estimated for all OLCI bands, and in each case, the algorithm architecture combines a minimal error with a minimal number of neurons. The neural network additionally inputs the solar geometry to allow for more accurate  $\langle K_d \rangle_1$  retrieval.



The non-water absorption coefficient,  $a_{nw}(\lambda)$ , and particulate backscattering,  $b_{bp}(\lambda)$ , coefficients are estimated from  $a(\lambda)$  and  $b_b(\lambda)$  for which the pure sea water absorption and backscattering coefficients have been removed. The  $a_w(\lambda)$  and  $b_{bw}(\lambda)$  values are estimated from Mason et al. (2016) and Zhang et al. (2009), respectively. The implementation of the Temperature and Salinity dependence of  $b_{bw}(\lambda)$  is done following Werdell et al. (2013).

The calculation of  $Y$  is done through a linear regression analysis between  $\text{Log}(b_{bp}(\lambda))$  and  $\text{Log}(\lambda)$ . For that purpose, only the  $b_{bp}(\lambda)$  values at 443, 490, 510 and 560 nm are used.

### 3.3 Water classification approach

The optical water classes (OWC) considered are based on the work of Melin & Vantrepotte (2015) where they applied a classification method of waters with a broad range of bio optical properties. Sixteen OWC were initially defined by these authors in their initial paper, an additional 17<sup>th</sup> optical class has then been added in order to take into account the ultra-oligotrophic waters of the oceanic gyres. These OWC were defined by Mélin and Vantrepotte (2015) considering a training data set of normalized  $R_{rs}$  spectra (Figure 1).

The classification then consists in calculating the class membership of a given  $R_{rs}$  spectrum to each of the 17 OWC which is defined statistically by its average spectrum,  $\mu$  (normalized and log transformed reflectance data), and a covariance matrix,  $\Sigma$ .

$$r_n = \frac{R_{rs}}{\int_{\lambda_1}^{\lambda_2} R_{rs} d\lambda}$$

Then, the classification method calculates the distance between the log value of the normalized input spectrum ( $x = \log(r_n)$ ) and the given class  $ic$  using the squared Mahalanobis distance  $\Delta_{ic}^2$ :

$$\Delta_{ic}^2(x) = (x - \mu_{ic})^T \sum_{ic}^{-1} (x - \mu_{ic})$$

where T indicates the matrix transpose. As a first approximation, this distance was used to quantify the proximity between an unknown  $R_{rs}$  spectra  $x$  and the  $R_{rs}$  data sets corresponding to the different optical classes defined in Mélin and Vantrepotte (2015),  $\mu_{ic}$ . It has to be compared to a theoretical threshold ( $\Delta_T^2$ ) provided from the Chi-square distribution which represents a given percentage of the data distribution for a degree of freedom corresponding to the dimension  $d$  (i.e. the number of wavelengths considered for testing the correspondence

between satellite  $R_{rs}$  spectra and those associated with the referenced optical classes (Vantrepotte et al. (2012)).

Note that an accurate estimation of the class membership probability associated with an unknown spectrum (like through the fuzzy logic approach described in Moore et al., 2001, Mélin and Vantrepotte 2015) would provide more precise information, particularly useful in deriving class based inversion algorithms using OWCs.

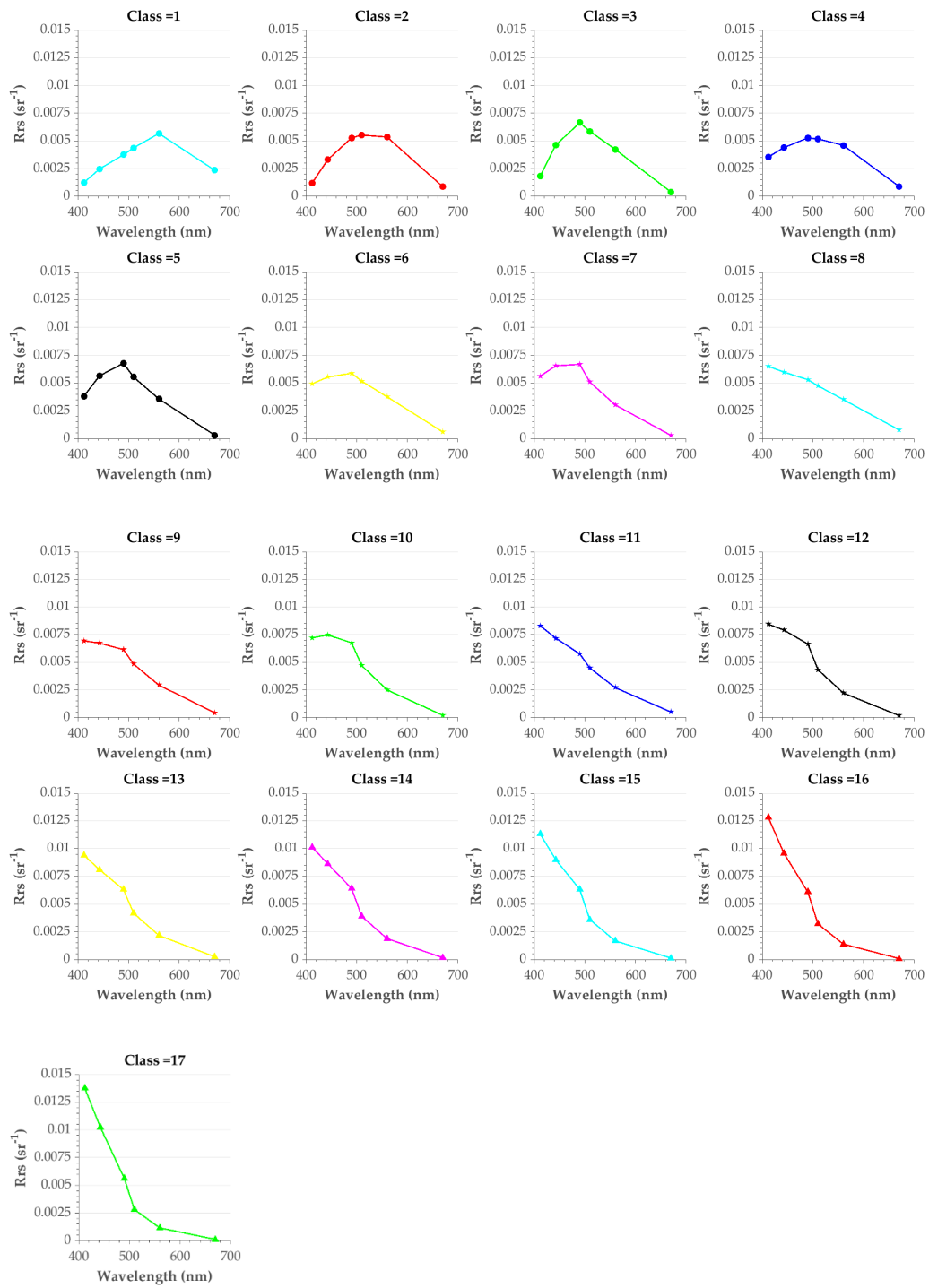


Figure 1: Illustration of the mean spectrum associated with the 17 OWT considered in the frame of this study (16 from Mélin and Vantrepotte, 2015 + 1 OWT for gyre area). Unclassified spectra are flagged as class -1.

### 3.4 Estimation of the absorption by phytoplankton and colored dissolved organic matter

The step 2 inversion is based on the model of Zhang et al. (2015) in which  $a_{nw}(\lambda)$  is fractioned into  $a_{phy}(\lambda)$  and  $a_{cdm}(\lambda)$ , where specific absorption  $a_{phy}^*$  is further decomposed in three size classes: micro, nano and picoplankton. For each phytoplankton size class, the specific absorption spectrum is assumed from Uitz et al. (2008). For  $a_{cdm}$  the authors assumed the specific absorption spectra normalized at 400 nm as wavelength-dependent exponential  $a_{cdm}^* = e^{(-S(\lambda-400))}$ . Consequently,

$$a(\lambda) = \sum_{i=1}^M m_i a_i^*(\lambda)$$

where M is the number of constituents,  $a_i^*(\lambda)$  is the specific absorption of constituent  $i$  at  $\lambda$  (eigenvector), and  $m_i$  is its specific contribution (eigenvalue). The eigenvectors were constructed to avoid either singularity or ill-condition, which requires that for any given  $a_i^*$  the difference to the other constituents ( $a_j^*$ ) is beyond a certain threshold. For this algorithm, the threshold  $S_{i,j}$  was set at 0.1 and is calculated as follows:

$$S_{i,j} = \frac{2}{BN} \sum_{k=1}^{BN} \left| \frac{a_i^*(\lambda_k) - a_j^*(\lambda_k)}{a_i^*(\lambda_k) + a_j^*(\lambda_k)} \right|$$

where BN stands for band number. The authors used a non-negative optimization scheme to obtain the absorption fractions, and this process can be done in two different ways based on which OWC the  $R_{rs}$  spectrum belongs to. First, the  $a_{cdm}(\lambda)$  slope (S) is estimated from the  $a_{nw}$  as originally done in Zhang et al. (2015) for OWC 1 and 2. For OWC between 3 and 17, S is directly calculated using a similar equation as developed in Lee et al. (2009) which has been slightly adapted for 2SAA :

$$S_{cdm} = 0.019 + \left( \frac{0.002}{0.6 + r_{rs}(443)/r_{rs}(560)} \right)$$

where  $r_{rs}$  is the remote sensing reflectance bellow water which is linked to  $R_{rs}$  as follows:  $r_{rs} = R_{rs}/(0.52+1.7R_{rs})$ .

In the second part of the algorithm, a single value decomposition (SVD) is used to optimize the eigenvalues and extract the corresponding fractions. The algorithm uses the proposed eigenvectors (specific absorption spectra) to extract chlorophyll-a for each size class and  $a_{cdm}$  at reference wavelength. From the chlorophyll-a and the specific absorptions spectrum, the model can reconstruct  $a_{phy}$ . A distinct characteristic of Zhang et al. (2015) model is the use of a non-negative optimization, in which all the solutions are feasible. The model

can use  $R_{rs}$  at any number of wavelengths as input during the optimization, and will give the full spectrum as output. For this optimization, the bands 412, 443, 490 and 510 proved to be the most accurate. Lastly the algorithm reconstructs  $a_{phy}$  in two different ways. If the class is 14 or below, the Zhang et al. (2015) optimization is used, and the  $a_{phy}$  is the sum of  $a_{phy}$  of each size class, otherwise  $a_{phy}$  is estimated by subtracting  $a_{cdm}$  from  $a_{nw}$ . This procedure is required because of the low values of  $a_{phy}$  in very oligotrophic waters (Bricaud et al. 2010), typically in gyres, and the higher sensitivity to noise in the inversion of  $a_{phy}$  compared to  $a_{cdm}$ .

### 3.5 Estimation of the colored dissolved organic matter

The last output generated in the proposed model is  $a_{cdom}(443)$ , based on the algorithm described in Loisel et al. (2014). The algorithm assumes that  $K_d(443)$  is mainly driven by the absorption coefficient. So, for wavelengths in which the absorption by CDOM is dominant, we can describe  $K_d$  as follows:

$$K_d(443) = K_w(443) + f(a_{cdom}(443)) + \Delta_p(443)$$

where  $K_w(443)$  is the diffuse attenuation coefficient for a pure sea water body,  $f(a_{CDOM}(443))$  is a function that only depends on the absorption coefficient by CDOM at 443 nm, and  $\Delta_p(443)$  is the residual term accounting for impact of scattering and absorption of particulate matters on the  $K_d(443)$  values.

The effect of particulate scattering and absorption on  $K_d(443)$  can be partially assessed using an appropriated wavelength, at which colored dissolved organic matter has a negligible or limited effect due to the dominating impact of pure sea water and particulate IOPs. In this case, the wavelength chosen is 560nm. As such, based on the equation previously described, a fit was constructed between the attenuation dominated by the effect of CDOM ( $X$ ) and the  $a_{CDOM}$  at 443 nm. For this algorithm, a linear fit performed on the IOCCG in situ data set was the most adequate, and it can be defined as:

$$a_{CDOM}(443) = 10^{[a1 \log_{10}(X) + b1]}$$

where  $a1$  and  $b1$  are equal to 0.9902 and -0.0522, respectively,  $X = Y - (\Delta_p(443) - \Delta_p(560))$  and  $Y = (K_d(443) - K_w(443)) - (K_d(560) - (K_w(560)))$

The term  $X$  is retrieved by dividing the equation in two parts, the contribution from  $K_d$  and  $K_w$  (term  $Y$ ), and the contribution from  $\Delta_p$ . The calculation of the term  $Y$  is done using a neural network approach based on Loisel et al. 2018 and Jamet et al. 2012, meanwhile the term  $\Delta_p(443) - \Delta_p(560)$  is calculated as follows:

$$\Delta_p(443) - \Delta_p(560) = 10^{[a2 \log_{10}(Y) + b2]}$$

where  $a_2$  and  $b_2$  are equal to 0.906 and -0.5259 respectively, and  $Y$  is the term estimated by the neural network.

#### 4 CRITERIA APPLIED TO CONSIDER A PIXEL VALID

During the implementation of the algorithm, different criteria were used to consider the pixel valid or not. For the first step of the inversion (LS2), the following criteria are used, otherwise the pixel is set as flagged, and no output is given for  $a_{nw}$  and  $b_{bp}$ :

- The input  $R_{rs}$  at 443, 490, 510 and 560 nm need to be positive.
- Retrieved  $K_d$  need to be positive for all wavelengths.

For the  $Y$  product, the value of  $R^2$  and the Significance Level based on the value of  $R$  and the degrees of freedom will be provided to the user as a parameter of uncertainty.

For the second step of the algorithm, the criteria are specific to the Zhang et al. (2015) algorithm. The optimization is done using a non-negative linear optimization, in which only positive values for  $a_{cdm}$  (443) and Chlorophyll-a are accepted. Another criteria used during the optimization is the tolerance between the input  $a_{nw}$  and the reconstructed  $a_{nw}$ , which was set at  $1 \cdot 10^{-4}$ .

Lastly, a final set of criteria is used for all the retrieved parameters. The  $R_{rs}$  is reconstructed following Werdell et al. (2013) and the thresholds are set as such:

- $-0.05 < b_{bp} < 1$
- $-0.05 < a_{cdm} < 10$
- $-0.05 < a_{phy} < 5$
- $\Delta R_{rs} < 33\%$

where  $\Delta R_{rs}$  is calculated as follows:

$$\Delta R_{rs} = \frac{100\%}{N_\lambda} = \sum_{i=1}^{N_\lambda} \frac{|\hat{R}_{rs}(\lambda_i) - R_{rs}(\lambda_i)|}{R_{rs}(\lambda_i)}$$

where  $\hat{R}_{rs}(\lambda_i)$  is the reconstructed  $R_{rs}$  at the wavelength  $i$ , and  $R_{rs}(\lambda_i)$  is the measured  $R_{rs}$  at wavelength  $i$ . The value of  $\Delta R_{rs}$  is provided as a standard product, allowing the end-user to have a certain confidence in the inversion process.

A table with all the flags used in 2SAA can be seen below:

Table 1 Specific flags for each parameter described in this section.

Flag name	Flag condition	Flag output
R <sub>rs</sub> failure	$\Delta R_{rs} > 33\%$	1
b <sub>bp</sub> Failure	$-0.05 > b_{bp} > 1$	2
a <sub>cdm</sub> Failure	$-0.05 > a_{cdm} > 10$	4
a <sub>phy</sub> Failure	$-0.05 > a_{phy} > 5$	8
K <sub>d</sub> Failure	$K_d < 0$	16

## 5 REFERENCES

- Bricaud, A., Babin, M., Claustre, H., Ras, J. and Tièche, F., 2010. Light absorption properties and absorption budget of Southeast Pacific waters. *Journal of Geophysical Research: Oceans*, 115(C8).
- Jamet, C., Loisel, H. and Dessailly, D., 2012. Retrieval of the spectral diffuse attenuation coefficient K<sub>d</sub> (λ) in open and coastal ocean waters using a neural network inversion. *Journal of Geophysical Research: Oceans*, 117(C10).
- Lee, Z., Lubac, B., Werdell, J. and Arnone, R., 2009. An update of the quasi-analytical algorithm (QAA\_v5). *International Ocean Color Group Software Report*, pp.1-9.
- Loisel, H. and Stramski, D., 2000. Estimation of the inherent optical properties of natural waters from the irradiance attenuation coefficient and reflectance in the presence of Raman scattering. *Applied optics*, 39(18), pp.3001-3011.
- Loisel, H., Vantrepotte, V., Dessailly, D. and Mériaux, X., 2014. Assessment of the colored dissolved organic matter in coastal waters from ocean color remote sensing. *Optics Express*, 22(11), pp.13109-13124.
- Loisel, H., Stramski, D., Dessailly, D., Jamet, C., Li, L. and Reynolds, R.A., 2018. An Inverse Model for Estimating the Optical Absorption and Backscattering Coefficients of Seawater From Remote-Sensing Reflectance Over a Broad Range of Oceanic and Coastal Marine Environments. *Journal of Geophysical Research: Oceans*, 123(3), pp.2141-2171.
- Mason, J.D., Cone, M.T. and Fry, E.S., 2016. Ultraviolet (250–550 nm) absorption spectrum of pure water. *Applied optics*, 55(25), pp.7163-7172.
- Mélin, F. and Vantrepotte, V., 2015. How optically diverse is the coastal ocean?. *Remote Sensing of Environment*, 160, pp.235-251.

Uitz, J., Huot, Y., Bruyant, F., Babin, M. and Claustre, H., 2008. Relating phytoplankton photophysiological properties to community structure on large scales. *Limnology and Oceanography*, 53(2), pp.614-630.

Vantrepotte, V., Loisel, H., Dessailly, D. and Mériaux, X., 2012. Optical classification of contrasted coastal waters. *Remote Sensing of Environment*, 123, pp.306-323.

Werdell, P.J., Franz, B.A., Lefler, J.T., Robinson, W.D. and Boss, E., 2013. Retrieving marine inherent optical properties from satellites using temperature and salinity-dependent backscattering by seawater. *Optics express*, 21(26), pp.32611-32622.

Zhang, X., Hu, L. and He, M.X., 2009. Scattering by pure seawater: effect of salinity. *Optics Express*, 17(7), pp.5698-5710.

Zhang, X., Huot, Y., Bricaud, A. and Sosik, H.M., 2015. Inversion of spectral absorption coefficients to infer phytoplankton size classes, chlorophyll concentration, and detrital matter. *Applied optics*, 54(18), pp.5805-5816.